Dynamics of Excitons in Single Semiconductor Quantum Dots Probed by Time-Resolved Optical Spectroscopy

D. V. Regelman (a), E. Dekel (a), D. Gershoni (a), W. V. Schoenfeld (b), and P. M. Petroff (b)

(a) Physics Department, Technion–Israel Institute of Technology, Haifa 32000, Israel

(b) Materials Department, University of California, Santa Barbara, CA 93106, USA

We resolve spatially, spectroscopically and temporally the photoluminescence emission from single self-assembled In(Ga)As/GaAs quantum dots. The temporal evolution of the emission spectrum after pulsed excitation is measured for various excitation intensities at various ambient temperatures. The evolution of the spectrum with the increase in both steady state and pulse excitation intensities is measured as well. A multi-exciton model is used for calculating the temporal and excitation intensity dependence of the measured spectra. The quantitative agreement between the measured and calculated spectra provides an unambiguous determination of the radiative lifetime of a single quantum dot exciton. This lifetime is 4–6 ns long and is temperature independent. The reduced spatial coherence between the confined exciton and the radiation electromagnetic field quantitatively explains this long radiative time.

Optical studies of semiconductor quantum dots in general and self-assembled quantum dots (SAQDs) in particular [1–6] have been a subject of very intensive recent investigations. These investigations brought strong spectral evidences that the presence of few confined carriers in the small volume of a QD give rise to correlated few carrier multiplexes, which are unstable otherwise. It has been shown that the number of carriers which occupy the photoexcited QD greatly affect the photoluminescence (PL) spectrum. Specifically, it has been established that Coulomb exchange terms between carriers of same charge are instrumental for the understanding of the measured PL spectra, when more than two excitons participate in the radiative process [5–10].

In this study, we present temperature dependent continuous wave (cw) and time-resolved spectroscopical studies of the recombination processes of photogenerated carriers in single In(Ga)As/GaAs SAQDs. The hosting layers of these dots, unlike those of our previous studies [5, 6] contain no aluminum. Therefore, their non-radiative decay rates are greatly reduced [11], and their enhanced PL makes it easier to facilitate time-correlated single-photon counting techniques [12–14].

The theoretical model which we have previously developed [5, 6, 9] is used here to quantitatively analyze our low light level time-resolved PL measurements. The quantitative analysis determines the radiative decay rates of the correlated multiexcitons.

The SAQD sample was grown by molecular beam epitaxy of a strained epitaxial layer of InAs on (100) oriented GaAs substrate. Small islands of In(Ga)As connected by a very thin wetting layer are thus formed. The vertical and lateral dimensions of the InAs SAQDs were adjusted during growth by the partially covered island growth technique [15]. The uncapped dots were found to have base dimensions of 45 nm by 40 nm and height of 4.5 nm by the use of atomic force microscopy. The sample was not ro-

tated during the growth of the SAQD layer, therefore a gradient in the QDs density was formed and low density areas, in which the average distance between neighboring QDs is larger than our optical spatial resolution, could be located on the sample surface. We use diffraction limited temperature variable confocal optical microscope for the PL studies of the single SAQDs [6]. For time-resolved spectroscopy the dispersed light from the monochromator was focused onto a thermo-electrically cooled, avalanche silicon photodiode. The signal from the photodiode was analyzed using conventional photon counting electronics. We locate an optically excited SAQD by scanning the sample surface while monitoring the resulted PL spectra. Once a typical emission spectrum from a SAQD is observed, the scan is terminated and the objective position is optimized above the dot. In Fig. 1a we display typical PL spectra from a single SAQD for various cw excitation powers at photon energy of 2.25 eV. At the lowest excitation density (0.01 μW), a single narrow spectral line is observed at energy of 1.284 eV. We denote this line by A_1. Its linewidth at this excitation density is limited by the spectral resolution of our system (0.2 meV). As the excitation density increases, two notable changes in the PL spectrum occur: first, a satellite spectral line (A_2) appears 3.5 meV below A_1. Second, a higher energy spectral line (B_1) emerges at 1.324 eV, 40 meV above the line A_1. At yet higher excitation power, an additional spectral line (B_2), develops 1.5 meV lower in energy than B_1. Further increase in the excitation power results in an increase in the number of satellites, gradually forming spectral PL bands to the lower energy side of the lines A_1 and B_1, respectively. In addition, new higher energy groups of spectral lines (C, D and E) gradually emerge and similarly develop their own satellites and lower energy spectral bands. With the increase in power, all the
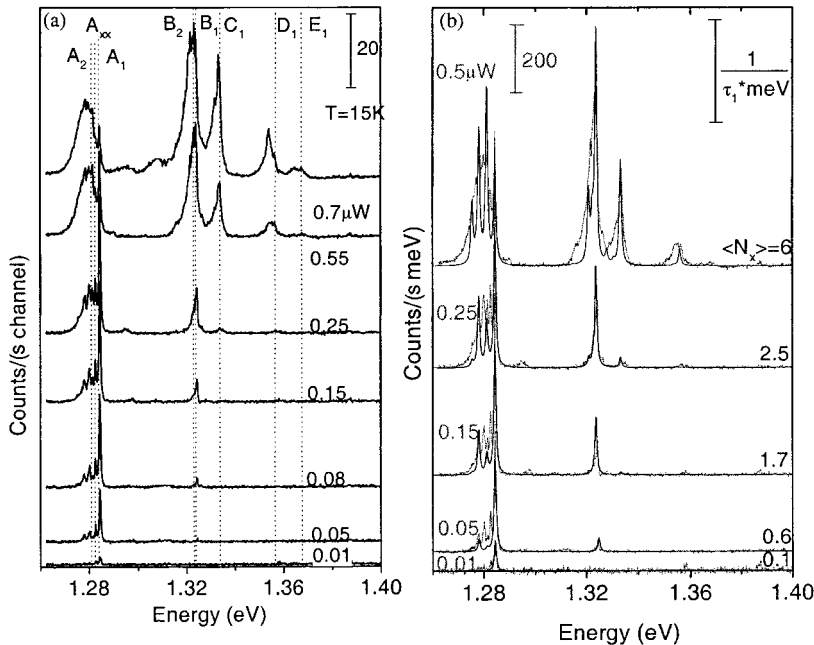

Fig. 1. a) Measured and b) calculated single SAQD PL spectra at various cw excitation powers. The spectra are vertically shifted for clarity
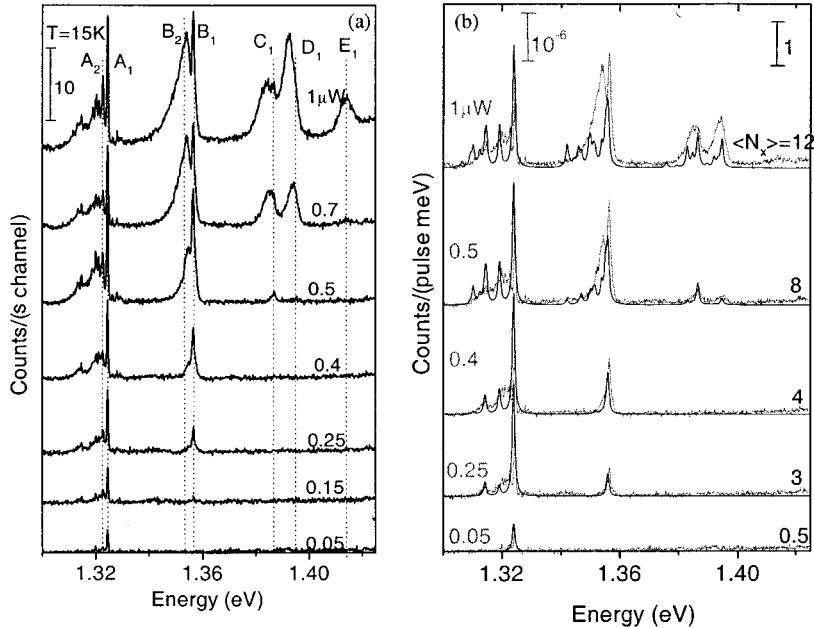
Fig. 2. a) Measured and b) calculated single SAQD PL spectra at various pulse excitation powers. The curves are vertically shifted for clarity

observed lines at their appearance order, undergo a cycle in which their emission intensity first increases, then reaches maximum and saturates, and eventually, at yet higher excitation power, significantly weakens. Consequently, the various groups seem to be "red shifted" with the increase in excitation power. Our model simulations, presented for comparison in Fig. 1b, duplicates this behavior.

In Fig. 2a we present PL spectra from a single SAQD for various excitation powers by picosecond short 1.750 eV laser pulses. The spectra as measured in this case represent temporal average on the PL emission. Their evolution with increasing excitation power is similar to that observed in the cw excitation mode (Fig. 1a), except for one significant difference: with the increase in excitation power, after reaching saturation, the intensity of the PL from the various spectral lines remains constant and it does not decrease with further increase in the excitation power. Our model simulations [5, 6, 9] for this case are presented for comparison in Fig. 2b.

In Fig. 3a we present the PL intensity of the single SAQD spectral line A_1 as a function of time after the excitation pulse. The PL transients were measured at 70 K for various excitation powers. In general, for each spectral line there are two distinct time domains. In the first, the emission intensity rises and in the second, it decays. As a rule we noted (not shown) that the lower the energy of a given spectral group of lines is, the longer are their rise and decay times. Within a given group of lines, however, lower energy lines rise and decay faster. The rise time of a particular spectral line strongly depends on the excitation power. The higher the power is, the longer is the rise time, while the decay time is hardly affected. Our model calculations [5, 6, 9] are presented for comparison in Fig. 3b. In the inset to Fig. 3a we display by symbols the measured
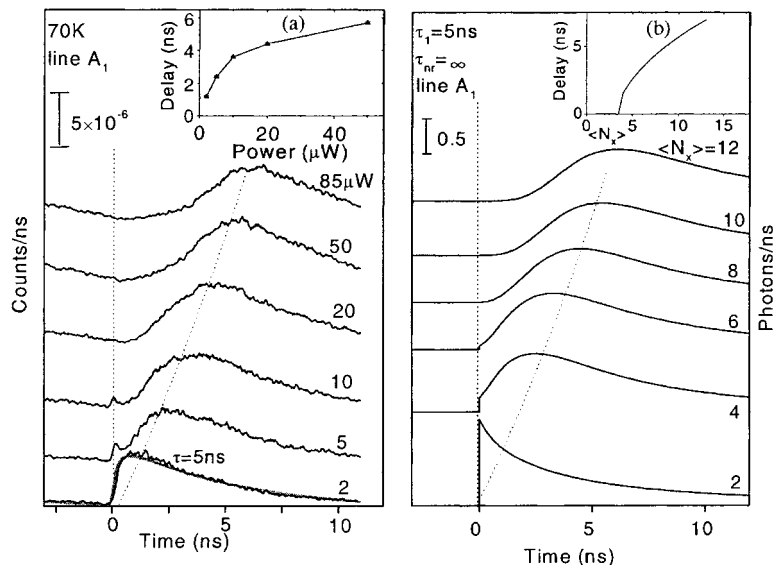
Fig. 3. The intensity of line A_1 from SAQD vs. time at 70 K. a) (b)) Measured (calculated) for various powers ($\langle N_x \rangle$ values). The inset displays the measured (calculated) rise time of the PL vs. the excitation power ($\langle N_x \rangle$)

rise time of the spectral line A_1 as a function of the excitation power. Our model calculations are presented for comparison in the inset to Fig. 3b.

The emission spectrum of a photoexcited quantum dot results from the radiative annihilation of multicarrier states. In previous works we showed that this spectrum can be quite well approximated provided that the energy levels of single carriers within the dot are known and that the exchange energies between these levels are known as well [5, 6, 9]. In order to calculate these energies, an exact knowledge of the quantum dot dimensions, geometrical shape, composition and strain field is required [16, 17]. At this stage, it is unrealistic to expect such a detailed knowledge for each SAQD. Fortunately, these energies can be, to a large extent, deduced directly from the measured QD emission spectrum. For example, it is quite obvious that the single line that we observe at low excitation density (line A_1) is due to the recombination of a single exciton within the optically excited SAQD. Similarly, it follows that the first line in the higher energy group of spectral lines (line B_1) is due to the recombination of an electron–hole (e–h) pair in their respective second energy levels. Lines (C_1) and (D_1) similarly mark higher energy optical transitions due to the recombination of e–h pairs at their respective third and fourth single carrier energy levels, respectively. As we demonstrated in Ref. [5, 6, 9] the combined e–e and h–h exchange energy between their first and second single carrier levels is given precisely by the energy difference between line A_1 and line A_2. Similarly, the energy difference between the spectral lines B_1 and B_2 is an exact measure for the combined exchange energy between the first and third single carrier energy states.

The e–e and h–h exchange interactions are responsible for the line splitting described in Figs. 1a and 2a. In addition, they give rise to a spectral red shift of optical transitions from successively higher order multiexcitons. As we demonstrated previously

[5, 6, 9], this red shift is caused by the number of exchange interactions, which increases with the number of participating carriers.

In order to calculate the PL spectrum a knowledge of the recombination rates of all multiexcitons is required. Exact calculation of these rates requires exact knowledge of the confined single carrier wave functions. Again, this is unrealistic to expect. We choose to estimate these rates using the following simplifications: only optical transitions in which a photon is emitted as a result of the annihilation of one e–h pair is considered. We use the dipole approximation for calculating the optical transition rate between initial and final multiexcitonic states and we assume that the dipole matrix element for optically allowed transitions between single carrier states is equal to that of the single exciton [5, 6]. Finally, only optical transitions between multiexciton states of same total spin and same spin projection along the growth axis are considered [5–7]. The optical recombination rates are then easily estimated by counting the number of angular momentum and symmetry conserving transitions between the initial to the final states. We assume that a multiexciton reaches thermal equilibrium and relaxes to its ground level much faster than its recombination rate. Therefore, only optical transitions from the ground energy level of each $(N + 1)$-th multiexciton to all possible levels of the N-th multiexciton are considered. Now, we use the estimated radiative recombination rates as input values to a set of coupled rate equations which describes the recombination of various multiexcitons within a QD. These equations are analytically solved for the cw as well as for the pulse excitation. The solutions yield the various probabilities of finding multiexcitons within the photoexcited QD [9]. Finally, we use the calculated multiexciton energies (spectrally broadened by a Gaussian of 0.5 meV width), their probabilities and the optical transition rates between them for simulating the PL emission spectra presented in Figs. 1b and 2b. The calculated temporal evolution of the PL emission from the A_1 spectral line for various initial numbers of e–h pairs ($\langle N_x \rangle$) is described in Fig. 3b.

As can be seen by comparison between the measured spectra and the calculated ones, our calculations mimic the experimental observations quite well. In particular, the rise time of the various spectral lines and its dependence on the excitation intensity, is quantitatively given by our model (see for example the inset to Fig. 3b, for the A_1 line). This increase in the rise time with the excitation intensity can be intuitively understood recalling that this rise time is actually the time it takes for the photogenerated N_x e–h pairs to recombine such that the QD is left with only up to three e–h pairs. This is because recombination from higher occupation levels do not contribute to the A_1 PL line [5, 6, 9].

From the comparison between the measured and calculated rise time as a function of the excitation intensity the QD single exciton lifetime can be straightforwardly deduced. The lifetime that we obtain amounts to 4–6 ns. The same lifetime is independently obtained from the comparison between the calculated and measured cw and pulsed temporally integrated spectra of Figs. 1 and 2, respectively.

It worth noting that the PL decay time of the A_1 line at 70 K (τ in Fig. 3a), is (5 ± 1) ns long, merely equals the radiative time. This means that at this temperature (unlike the situation at lower temperatures [9]) the SAQD single exciton decay is almost purely radiative.

The temperature independent lifetime that we obtained is an order (two orders) of magnitude longer than the intrinsic radiative lifetime of single excitons confined in

semiconductor quantum wires [18–20] (quantum wells [21, 22]). Following the arguments of Andreani [21], and Citrin [18] who calculated the intrinsic radiative lifetimes of single excitons in semiconductor QWs and QWRs, respectively, we find for excitons in spherical QDs: $\tau_0^{QD} = nm_0c/e^2fk_{ex}^2$, where n, m_0, e and c are the material index of refraction, electronic mass, electron charge and speed of light, respectively, f is the confined exciton oscillator strength and $k_{ex} = n\omega/c$ is the exciton wavevector in the material. For exciton energy $\hbar\omega = 1.35$ eV and $f = 0.5$ for QDs of these dimensions [23], we get $\tau_0^{QD} = 4.2$ ns, in reasonable agreement with our temperature independent experimental findings. We therefore conclude that the long quantum dot single exciton radiative lifetimes that we measured are due to the reduced spatial coherence between the confined exciton dipole moment and the extended electromagnetic radiation field.

References

[1] M. Bayer et al., Phys. Rev. B **58**, 4740 (1998).
[2] A. Zrenner et al., Physica B **256–258**, 300, 356–358 (1998).
[3] L. Landin et al., Phys. Rev. B **60**, 16640 (1999).
[4] Y. Toda, O. Moriwaki, M. Nishioka, and Y. Arakawa, Phys. Rev. Lett. **82**, 4114 (1999).
[5] E. Dekel et al., Phys. Rev. Lett. **80**, 4991 (1998).
[6] E. Dekel et al., Phys. Rev. B **61**, 11009 (2000).
[7] A. Barenco and M. A. Dupertuis, Phys. Rev. B **52**, 2766 (1995).
[8] A. Wojs and P. Hawrylak, Phys. Rev. B **55**, 13066 (1997).
[9] E. Dekel et al., Phys. Rev. B **62**, (2000).
[10] R. Rinaldi et al., Phys. Rev. B **62**, 1592 (2000).
[11] I. Shtrichman, D. Gershoni, and R. Kalish, Phys. Rev. B **56**, 1509 (1997).
[12] U. Bockelmann, W. Heller, A. Filoramo, and Ph. Roussignol, Phys. Rev. B **55**, 4456 (1997).
[13] G. Bacher et al., Phys. Rev. Lett. **83**, 4417 (1999).
[14] V. Zwiller et al., Phys. Rev. B **59**, 5021 (1999).
[15] J. M. Garcia et al., Appl. Phys. Lett. **72**, 3172 (1998).
[16] L.W. Wang, J. Kim, and A. Zunger, Phys. Rev. B **59**, 5678 (1999).
[17] O. Stier, M. Grundmann, and D. Bimberg, Phys. Rev. B **59**, 5688 (1999).
[18] D. S. Citrin, Phys. Rev. Lett. **69**, 3393 (1992).
[19] H. Akiyama et al., Phys. Rev. Lett. **72**, 924 (1994).
[20] D. Gershoni et al., Phys. Rev. B **50**, 8932 (1994).
[21] L. C. Andreani, Solid State Commun. **77**, 641 (1991).
[22] B. Deveaud et al., Phys. Rev. Lett. **67**, 2355 (1991).
[23] T. Takagahara, Phys. Rev. B **39**, 10206 (1989).